


Article

# An Experimental Investigation of Wave Forces on a Submerged Horizontal Plate over a Simple Slope

Jie Dong <sup>1,2</sup>, Leiping Xue <sup>2,\*</sup>, Kaiyu Cheng <sup>1</sup>, Jian Shi <sup>3</sup>  and Chi Zhang <sup>3</sup>

<sup>1</sup> Powerchina Huadong Engineering Corporation Limited, Hangzhou 311122, China; dong\_j@ecidi.com (J.D.); cheng\_ky@ecidi.com (K.C.)

<sup>2</sup> School of Naval Architecture, Ocean and Civil Engineering, Shanghai Jiao Tong University, Shanghai 200240, China

<sup>3</sup> College of Harbor, Coastal and Offshore Engineering, Hohai University, Nanjing 210098, China; jianshi@hhu.edu.cn (J.S.); zhangchi@hhu.edu.cn (C.Z.)

\* Correspondence: lpxue@sjtu.edu.cn

Received: 4 June 2020; Accepted: 7 July 2020; Published: 9 July 2020



**Abstract:** We experimentally investigated the forces induced by monochromatic and solitary waves on a submerged horizontal plate in a wave flume. The experimental results of two-dimensional wave forces on the plate over a 1:10 simple slope and a flat bottom are presented. The effects of the uneven bottom on wave loads are discussed by comparing the results with those in a constant water depth. The measured nonlinear wave forces exhibited considerable discrepancies with the theoretical results from the linear wave theory. The wave forces on the plate induced by monochromatic waves over the simple slope in intermediate water showed no appreciable difference with the flat-bottom results. The solitary wave forces in terms of the downward vertical force and overturning moment significantly decreased in the existence of the simple slope. Furthermore, the dependency of the wave length, wave height and the submergence depth on the wave loads is also discussed.

**Keywords:** submerged horizontal plate; variable bottom topography; wave force; solitary wave

## 1. Introduction

A fully submerged horizontal plate is a common simplified type of many coastal and ocean engineering structures and is often suggested as a plate-type breakwater [1,2], semi-submersible very large floating structure (VLFS) [3], or plate-type wave energy converter (WEC) [4–6]. These plates can provide an economical solution for coastal areas with a minimum effect on nearshore current, sediment transport and so on. The wave reflection and transmission characteristics of a monochromatic wave on such a submerged breakwater have been widely investigated over recent decades [7–11]. The wave-induced load on a submerged plate due to the pressure differential is also an important subject for a number of scientific and engineering problems [12–14].

Linear wave theory has been applied to analyze the wave scattering by a submerged horizontal plate since the 1950s [1,2]. The reflection and transmission characteristics of monochromatic waves were obtained through analytical methods and numerical approaches. Siew and Hurley [7] presented an asymptotic solution of the reflection and transmission coefficients for long waves on an infinitesimally thin plate in a constant water depth. However, the nonlinear features associated with wave breaking, higher harmonics and vortexes are critical issues in the wave-plate problem. Yu et al. [15] proposed an inception condition for wave breaking over a submerged horizontal plate, which was based on an empirical formula for partial standing wave breaking in a uniform water depth. Linear and nonlinear wave forces exerted on a submerged horizontal plate were studied using an eigenfunction expansion (EFE) method, together with the perturbation technique up to the second order [16].

Liu et al. [17] discussed the main features of the generation and transmission of higher harmonics based on a desingularized boundary integral equation method and compared the numerical results with their experimental measurements. Poupardin et al. [18] showed detailed information of the flow and vortex field near the plate with particle image velocimetry (PIV) measurements. Yu et al. [19] reviewed the functional performance of a submerged horizontal plate and the effects of the plate width, the submergence depth, the porosity and the inclination of the plate. Other interesting subjects related to wave interactions with underwater structures similar to a plate have been discussed in previous studies [20–22].

Recently, adjective investigations used analytical, computational, empirical and experimental approaches to thoroughly understand the mechanisms of the wave transformation and the hydrodynamic loads on a submerged plate. Hayatdavoodi et al. [23,24] presented the results of solitary and cnoidal wave loads on a submerged deck in a constant water depth based on the level I Green–Naghdi (GN) equations and suggested two empirical equations for the design of a submerged deck. Dong et al. [25] proposed an approximate solution of linear wave loads on a submerged plate based on the linear potential flow theory and compared the theoretical results for different bottom types. A computational fluid dynamics (CFD) approach was also used to obtain the wave loads on a submerged plate [26,27]. Laboratory experiments of wave loads on a submerged, horizontal plate were conducted by, e.g., Wang et al. [28] and Jones et al. [29], who mainly focused on the behavior of a submerged plate under some specific conditions.

Although the scattering of regular waves on a submerged plate is widely studied, research on wave–plate interactions for other waveforms, such as solitary waves, is limited. Lo and Liu [30] investigated the interactions between a solitary wave and a submerged horizontal plate in shallow water. They presented the theoretical, experimental and numerical results of hydrodynamic loads on the plate for incident solitary waves on a flat bottom. Seiffert et al. [31] presented the results of the horizontal and vertical forces acting on a two-dimensional horizontal plate due to solitary waves by conducting a series of laboratory experiments, as well as CFD calculations. Hayatdavoodi et al. [32] studied solitary and cnoidal wave transformation over a submerged, fixed, horizontal rigid plate by using nonlinear GN equations in shallow water. A smoothed particle hydrodynamics (SPH) method was applied to evaluate the wave-induced loads on a submerged plate [33–35]. Ning et al. [36] investigated wave-induced loads on a submerged plate in uniform currents and discussed the coupling effect of waves and currents.

Much effort has been devoted to investigating the interaction of waves and a submerged horizontal plate for the conditions of uniform water depth. However, the hydrodynamic behaviors of the submerged plate in non-uniform water depth with an uneven bottom is of scientific significance, as well as of engineering importance. The pioneering work of investigating the behavior of water wave propagation over uneven bottoms was carried out by Madsen and Mei [37] and Dingemans [38]. Yet, the behavior of waves on a submerged horizontal plate over an uneven bottom remained an interesting issue. In most cases, these types of submerged structures were constructed in coastal zones, where the water depth is not constant but variable. For example, for a very large submerged plate-type breakwater or WEC device in the water of a coral reef region with variable bottom topography, the effect of varied water depth on the hydrodynamic loads should be taken into account. The wave-plate interaction problems with several typical bottom types, e.g., step bottom [39,40], sinusoidal ripples or Gauss-type curves [41], were studied using a simplified perturbation method.

In this paper, we present an experimental comparative study on wave scattering by a submerged horizontal plate over a 1:10 simple slope to evaluate the effects of an uneven bottom on the wave-induced forces. Both monochromatic and solitary waves were considered in the experiments. The effects of the uneven bottom on wave loads are discussed by comparing the results with those in constant water depth. The dependency of wave length, wave height and submergence depth on the wave loads is also discussed. The paper is organized as follows: The experimental set-up and the methodology for wave-induced force measurements are detailed in Section 2. In Section 3, the incoming wave conditions

of the monochromatic and solitary waves and wave generation are described and documented. The experimental data of the surface elevations and wave loads on a submerged plate over a flat and sloped bottom topography are presented in Section 4. The behavior of wave-induced forces with a simple slope are discussed for both the monochromatic and solitary waves and compared with linear solutions of the problem.

## 2. Experimental Set-Up

The experiments were carried out in a wave flume at the key laboratory of hydrodynamics in Shanghai Jiaotong University with a length of 60 m, a width of 0.8 m and a depth of 1.2 m. The water depth was set to be constant at 0.5 m. At one end of the flume, there was a piston-type wavemaker (Figure 1), and at the other end, a 1:10 porous slope was set up for wave absorbing, which reflected less than 3% of the incoming waves. The plate-type structure was made of organic glass with a length of 2 m, a width of 0.78 m and a thickness of 0.1 m. This structure was fixed by four aluminum struts attached to a rigid steel frame at the top of the flume, as shown in Figure 2. The aluminum struts were a V shape to minimize their influence on wave propagation on the plate. The steel frame was constructed from two parts, one was the part attached to the strut and the structure, and the other part was two beams that traversed the sidewall to support the frame in the wave flume. Four Karan pliers were used to fix the two parts, thus the submerged depth of the structure relative to the water surface could be adjusted freely by the steel frame. The gap between the plate and the sidewall of the wave flume was 1 cm. Therefore, wave forces exerted on the plate were assumed to be uniform along the width of the structure in the wave flume.

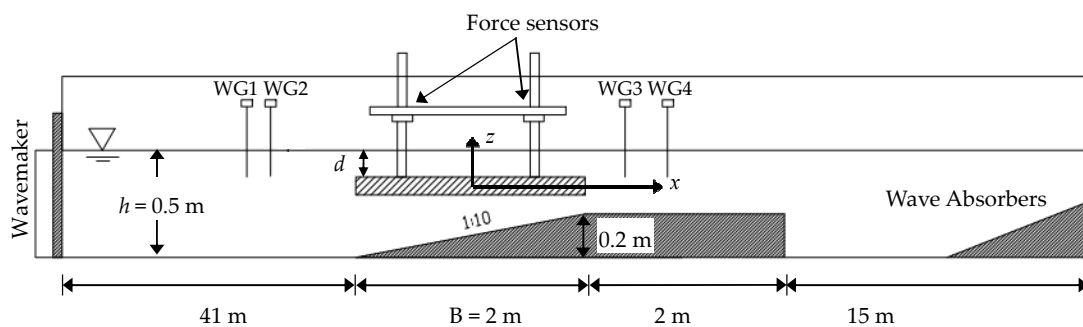


**Figure 1.** The sketch of the experimental set-up for a submerged horizontal plate of 2 m long and 10 cm thick over a simple 1:10 slope. Not to scale.

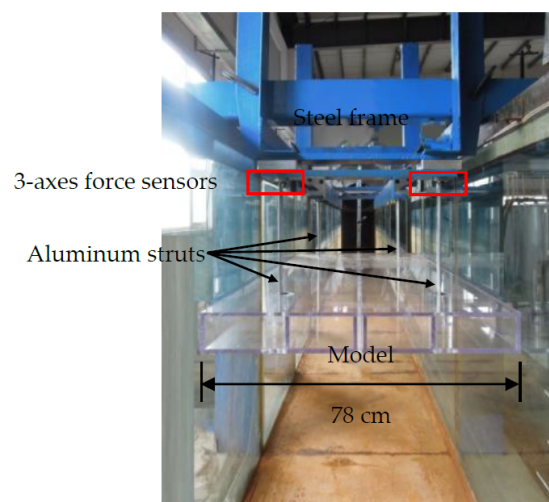


**Figure 2.** The model attached to the V-shape struts and connected to force sensors installed on a steel frame. The width of the leading edge of the model was 78 cm with a 1 cm gap at the sidewalls.

The force sensors were installed to connect the steel frame and each aluminum bar. Four K3D120 force sensors (ME-Measurement Systems GmbH) were used to measure the wave forces in the three directions of space and up to a 1 kN limit. The experimental data were processed by a computer with a National Instruments data acquisition card with a 1000 Hz sampling rate of data acquisition from the force sensors. The surface of the steel frame where the force sensors were affixed was specially smoothed in the workshop, to ensure that the four attached surfaces were in the same horizontal plane. The plate was carefully adjusted by an electronic gradienter before the experiments to ensure the plate was horizontal and in the centerline of the wave flume. After adjustments, the system was calibrated statically at an accuracy of 1% by given loads in the horizontal and vertical direction at different locations. The horizontal and vertical forces exerted on the structure were obtained by the sum of the recorded force component of each sensor. The center of the overturning moment was set at the center of the plate. Thus, the moment could be calculated by multiplying the force from each sensor with the corresponding distances. Hence, a dynamometric system was set up using the four force sensors and was able to measure the horizontal force, the vertical force and the overturning moment.

Resistance-type wire probes with amplifiers were installed in the front and in the rear of the structure, to record the water surface elevation. The wire probes had a nonlinearity of less than 1% and were carefully calibrated at an accuracy of 0.25%. There were two probes in the reflection region and two probes in the transmission region. The locations of the four wave gauges are listed in Table 1.

**Table 1.** The distances of wave gauges (WG) from the center of the model.

Wave Gauge	WG1	WG2	WG3	WG4
Coordinate on $x$ -axis <sup>1</sup>	−240 cm	−210 cm	170 cm	270 cm

<sup>1</sup> The definition of  $x$ -axis is illustrated in the following Figure 1.

A simple slope with a ratio of 1:10 was placed under the model in the slope cases, as shown in Figure 1. The length of the slope was equal to the length of the model along the flume and connected with a 2-m horizontal part in the transmission region. The frame of the slope bottom was made of Bakelite and was supported by the steel frame. To assure the impenetrability of the slope, the cavities at the tow of the slope and the joint of two Bakelite plates were filled with silica gel, and the gaps between the Bakelite plates and the sidewall of the wave flume were sealed with chemical foam.

### 3. Wave Conditions

#### 3.1. Regular Waves

Regular waves were generated by a sinusoidal motion of the piston-type wavemaker. A series of wave periods from 1.00 s to 2.20 s were chosen in the 0.50 m water depth. Thus, the wave length  $L$  ranged from 1.51 m to 4.53 m, which indicates these tests were in the intermediate water. The ratio  $L/B$  of wave length  $L$  to the plate length  $B$  is another important parameter, which was varied from 0.76 to 2.27. We observed that the amplitude of the waves decreased as a result of the viscosity and friction against the sidewall and bottom, by about 0.6% per wavelength. For example, for the case of ( $H = 0.10$  m,  $T = 1.2$  s), the input wave height for the wavemaker signal was 0.139 m, and so a regular wave with 0.10 m height was obtained at the plate location. The same tests of wave generation were conducted for each wave condition without the plate, and the target wave conditions were reproduced well in the wave flume. After several trials, three relative wave heights  $H/h = 0.10, 0.20$  and  $0.30$  were selected for the cases of regular waves.

The distance from the wavemaker to the model was 41 m. There were at least nine wave crests for the longest wave, i.e.,  $T = 2.20$  s and  $L = 4.53$  m. There was a time window when the leading part of the reflected wave train from the wavemaker had not yet reached the structure, and the measured surface elevations and forces were reasonably periodic. We used 7–10 wave periods in this window as the final time history of the surface elevation and forces. An illustration of the time histories of the

wave elevation and the corresponding force on the structure is provided in Figure 3. The actual time window we used was  $35 \text{ s} < t < 45 \text{ s}$ , i.e., about seven wave periods. The test cases of regular waves are shown in Table 2.

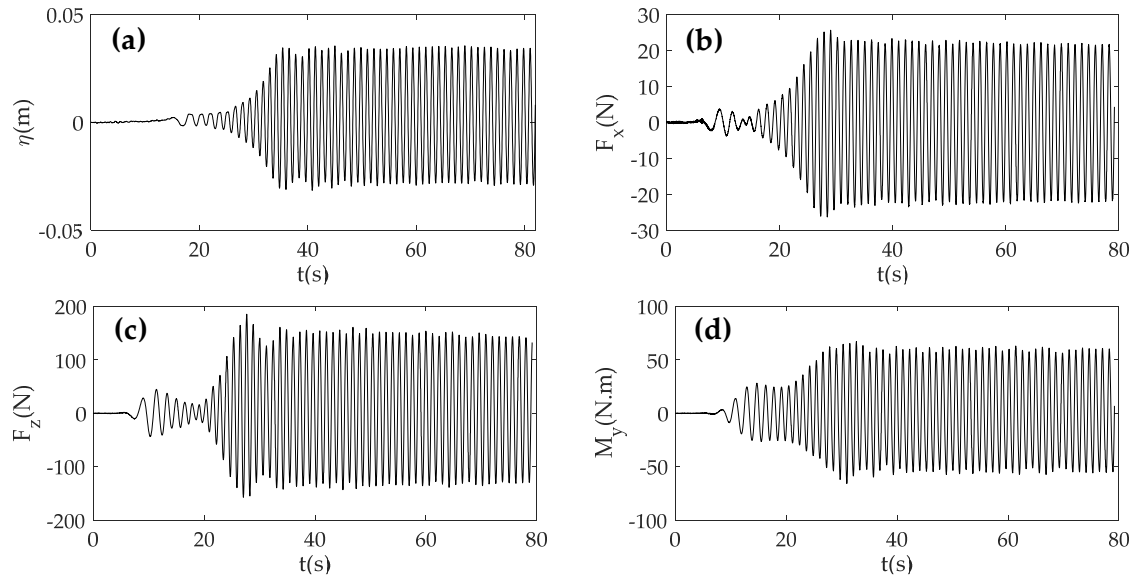


**Figure 3.** Samples of time series of (a) the surface elevation at WG1, (b) wave forces in the horizontal direction, (c) wave forces in the vertical direction and (d) overturning moments due to regular waves. ( $d = 0.14 \text{ m}$ ,  $h = 0.50 \text{ m}$ ,  $H = 0.05 \text{ m}$  and  $T = 1.2 \text{ s}$ ).

**Table 2.** Details of test cases of regular waves.

Case <sup>1</sup> (Flat vs. Slope)	Submergence Depth d (m)	Wave Height H (m)	Wave Periods T (s)
BF1 vs. BS1	0.140	0.05	1.20, 1.40, 1.60, 1.80, 2.00
BF2 vs. BS2	0.140	0.10	1.20, 1.40, 1.60, 1.80
BF3 vs. BS3	0.140	0.15	1.20, 1.40, 1.60, 1.80
BF4 vs. BS4	0.103	0.05	1.00, 1.20, 1.40, 1.60, 1.80, 2.00, 2.20
BF5 vs. BS5	0.103	0.10	1.00, 1.20, 1.40, 1.60, 1.80, 2.00, 2.20
BF6 vs. BS6	0.103	0.15	1.20, 1.40, 1.60, 1.80, 2.00
BF7 vs. BS7	0.076	0.05	1.00, 1.10, 1.20, 1.30, 1.40, 1.50, 1.60, 1.70, 1.80, 1.90, 2.00, 2.10, 2.20
BF8 vs. BS8	0.076	0.10	1.00, 1.10, 1.20, 1.30, 1.40, 1.50, 1.60, 1.70, 1.80, 1.90, 2.00, 2.20
BF9 vs. BS9	0.076	0.15	1.00, 1.10, 1.20, 1.30, 1.40, 1.50, 1.60, 1.70, 1.80

<sup>1</sup> BF indicates regular wave cases on a flat bottom and BS indicates cases on a sloped bottom.

### 3.2. Solitary Waves

An improved Goring wave generation methodology, as proposed by Malek-Mohammadi and Testik [42], was used to generate solitary waves in the wave flume. The new methodology is capable of generating more accurate solitary waves with less attenuation by taking the non-steady-state characteristics of piston-type wavemakers into account. Assuming that the horizontal water particle velocity adjacent to the wave paddle,  $u$ , is equal to the wave-paddle velocity,

$$\frac{dx}{dt} = u(x, t) \tag{1}$$

where  $x$  is the position of the wave paddle and  $t$  is the elapsed time since the start of the motion. Herein,  $u(x,t)$  is assumed to be constant throughout the water depth. Hence, the depth-averaged velocity  $u(x,t)$  is derived based on the conservation of mass and expressed for long waves of permanent form as

$$u(x,t) = \frac{c\eta(x,t)}{h + \eta(x,t)} \tag{2}$$

where  $\eta(x,t)$  is the free surface elevation above the still water level,  $h$  is the still water depth and  $c$  is the wave celerity.

In order to improve the accuracy of solitary waves with large amplitudes, the third-order solution proposed by Grimshaw [43] was implemented as the target profile of solitary waves in our experiments:

$$\eta(x,t) = Hsh^2 \left[ 1 - \frac{3}{4}\alpha th^2 + \alpha^2 \left( \frac{5}{8}th^2 - \frac{101}{80}sh^2th^2 \right) \right] \tag{3}$$

$$sh = \operatorname{sech}[k(ct - x)], \quad th = \tanh[k(ct - x)] \tag{4}$$

$$k = \sqrt{\frac{3H}{4h^3}} \left( 1 - \frac{5}{8}\alpha + \frac{71}{128}\alpha^2 \right), \quad c = \sqrt{gh} \left( 1 + \frac{1}{2}\alpha - \frac{3}{20}\alpha^2 + \frac{3}{56}\alpha^3 \right) \tag{5}$$

where  $H$  is the solitary wave height,  $\alpha$  is the relative wave height  $H/h$ ,  $g$  is the acceleration of gravity and  $k$  is the wavenumber.

The motion of the wavemaker was calculated from Equation (3) using the Newton–Raphson method. As mentioned above, there was a decrease in the solitary wave height; therefore, the actual solitary wave heights at the target location were measured in the wave flume without the structure. Figure 4 shows the measured time series of the surface elevation at the location of the probe WG1. This shows a good agreement between the measured surface elevation profile and the theoretical results. The relative solitary wave height we used in the following section was from 0.120 to 0.382, as shown in Table 3.

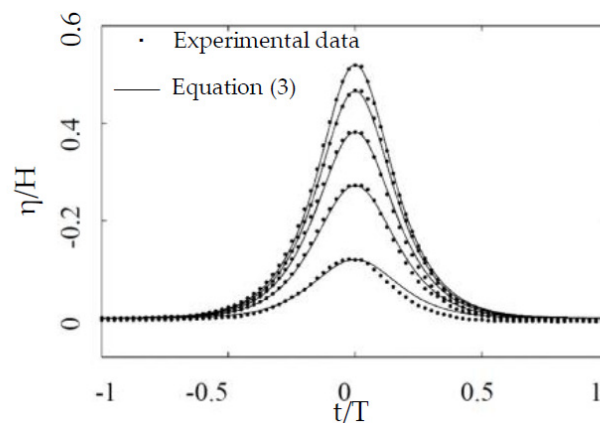


Figure 4. Time series of the surface elevation at the probe WG1 with different input solitary wave heights.

Table 3. Details of the test cases of solitary wave conditions.

Case <sup>1</sup> (Flat vs. Slope)	Submergence Depth d (m)	Wave Height H (m)
AF1 vs. AS1	0.140	0.060, 0.085, 0.110, 0.136, 0.163, 0.191
AF2 vs. AS2	0.103	0.060, 0.085, 0.110, 0.136, 0.163, 0.191
AF3 vs. AS3	0.076	0.060, 0.085, 0.110, 0.136, 0.163, 0.191

<sup>1</sup> AF indicates solitary wave cases on a flat bottom and AS indicates cases on a sloped bottom.

#### 4. Results and Discussion

In this section, we discuss regular waves and solitary waves. For each part, we first present the experimental results from a flat bottom in terms of the surface elevation and the wave forces. Then, the wave forces measured on a simple slope are compared with the results from a flat bottom so that the effects of the bottom topography on the wave forces are clearly illustrated.

##### 4.1. Regular Waves

The time series of surface elevation in the reflected and transmitted regions are plotted in Figure 5. The submergence depth was 14 cm, thus, the regular waves at a water depth of 50 cm were significantly deformed on the structure. We found that the higher harmonic components at the leading edge were much larger than those at the trailing edge of the plate. Higher harmonics were generated and propagated into the transmitted region. Wave components with high frequencies were observed at the rear of the model, as shown in Figure 5c,d.

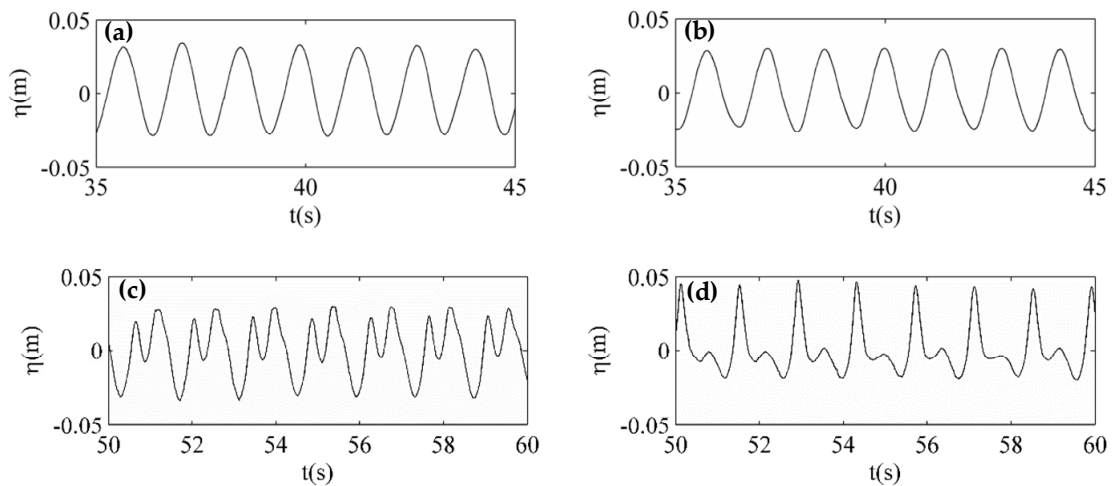


**Figure 5.** The time series of surface elevations in the front (a) WG1 and (b) WG2 and in the rear (c) WG3 and (d) WG4 of the plate under regular waves over a flat bottom. ( $d = 0.14$  m,  $T = 1.4$  s and  $H/h = 0.1$ ).

The corresponding wave forces and overturning moment are presented in Figure 6. The variations of the horizontal force, the vertical force and the overturning moment in the time window were basically static with the time. We found that variations of the wave force were nearly sinusoidal with relatively small wave lengths, e.g.,  $T = 1.2$  s; however, higher harmonic components became significant with increasing wave periods or wave length. In Figure 6b, significant higher-order components of the vertical force were observed. The amplitude of the horizontal force was far less than the vertical force, as the thickness of the plate is an important factor for horizontal force, while the length of the plate is important for vertical force.

Previous studies [10,24] showed that wave-induced loads on the plate were affected by water depth conditions and plate characteristics, including the wave height  $H$ , water depth  $h$ , plate length  $B$ , plate width  $W$ , plate thickness  $\delta$  and the submergence depth  $d$ . Specifically, the horizontal wave forces on the submerged plate were due to the pressure difference at the leading and trailing edges, while the vertical forces and consequent overturning moments mainly depended on the pressure difference on the upper and lower surfaces of the plate. The wave-induced pressure on the plate was consistent with the wave height  $H$  and was assumed as  $\rho gH$ , where  $\rho$  is the water density. Therefore, dimensionless wave-induced forces for regular waves are defined by the wave pressure and the contact area, i.e.,  $\delta \cdot W$

for the horizontal forces,  $B \cdot W$  for the vertical forces and  $B/2$  used as torque with respect to the middle of the plate for the overturning moment,

$$F_x^* = \frac{F_x}{\rho g H \delta W}, \quad F_z^* = \frac{F_z}{\rho g H B W}, \quad M_y^* = \frac{M_y}{0.5 \rho g H B^2 W} \quad (6)$$

where  $F_x$ ,  $F_z$  and  $M_y$  are dimensional amplitudes of the horizontal forces, vertical forces and overturning moments, respectively. The amplitude of wave forces in each direction was calculated by an average of the results of 7–10 wave periods in the chosen time window, as noted in Section 3.1.

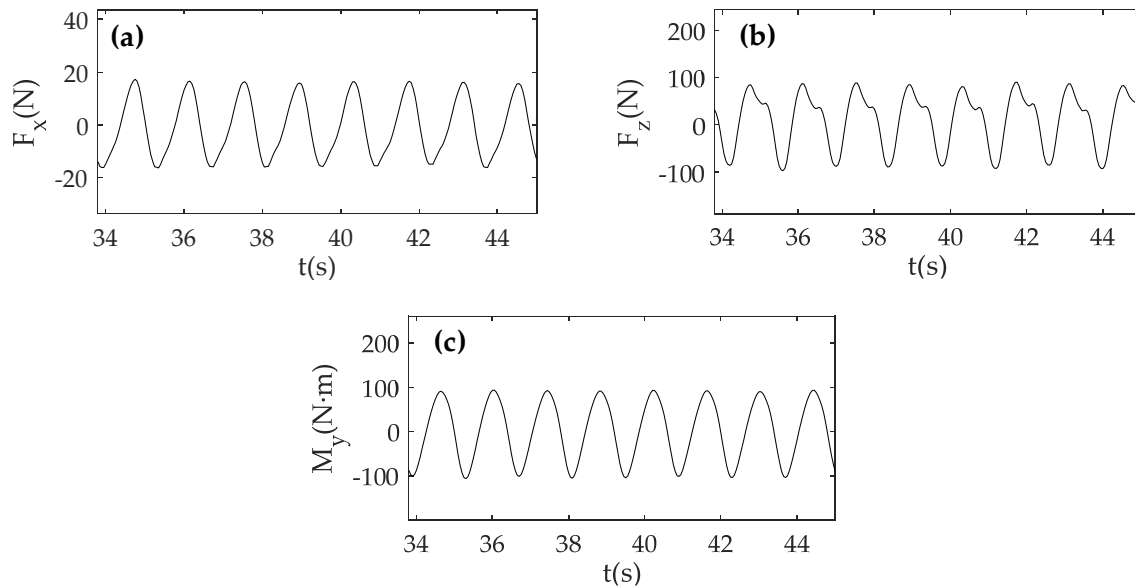


**Figure 6.** The time series of regular wave forces on a submerged horizontal plate over a flat bottom. ( $d = 0.14$  m,  $T = 1.40$  s and  $H/h = 0.10$ ). (a) Horizontal forces; (b) Vertical forces; (c) Overturning moments.

Variations of the dimensionless wave forces to the relative wavelength under regular waves on a flat bottom and a slope are shown in Figures 7–9. Herein, we define the relative wave length  $L/B$  as the regular wave length  $L$  ratio to the plate length  $B$ . From the experimental data, the wave forces in terms of the horizontal force, the vertical force and the overturning moment generally increased with the relative wave length, i.e., longer waves led to larger wave loads. However, there were slight decreases in specific cases; for example, the horizontal force in the range of  $1.0 < L/B < 1.8$  with  $H/h = 0.10$ , as Figure 7a shows. The wave forces increased gradually to a maximum value and no longer increased with the relative wave length. The overturning moment reached a maximum when  $L/B > 1.5$  with  $H/h = 0.10$ . The critical wave length appeared to be related to the relative wave height for the overturning moment. The overturning moment remained stable when  $L/B > 1.25$  for  $H/h = 0.20$  and  $L/B > 1.0$  for  $H/h = 0.30$ . The submerged depth had a weak influence on the horizontal force, which slightly decreased with the increasing submergence depth. The vertical forces and the overturning moment saw hardly any shift with the submergence depth, especially in the cases of relatively larger wave heights.

We found that the linear theory provided reasonable predictions when the relative wave height was 0.10 and the relative wave length was less than 1.5, as Figure 7a shows. For the incident wave with  $L/B > 1.5$ , a zero horizontal force was predicted by the linear theory, but the experimental data showed a slight decrease and then a gradual increase. The linear theory also overestimated the vertical forces and the overturning moment when  $L/B > 1.5$ . Patarapanich [12] stated the critical conditions for either zero horizontal or zero vertical forces, which were in fact identical to the conditions for no reflection.



The variation of pressure on the upper surface is sinusoidal in time and space, while the dynamic pressure distribution beneath the plate at any instant in a wave cycle was linear, as presented in [12,25].

When the wave length  $L$  was some particular ratio to the plate length  $B$ , the dynamic pressure on the upper and lower surfaces of the plate were able to cancel each other out, which led to zero forces. However, these conditions were strictly subjected to the linear long wave assumption. Wave breaking is an important phenomenon related to the nonlinearity and dissipation. In our experiments of regular waves, only in the case of  $H/h = 0.10$  and  $d/h = 0.280$ , did the wave not break when it propagated across the plate. For other cases of larger wave heights or shallower submergence depths, we observed that wave breaking occurred above the plate. For this reason, the effect of the submergence depth on wave forces was not obvious. The measured wave loads with different submergence depths were essentially consistent with different wave heights. For the cases where the relative wave heights were 0.20 and 0.30, the linear theory failed to predict the wave forces well due to the strong nonlinearity effects.

The experimental results for the wave forces over a simple slope are also presented with different submergence depths and relative wave heights for comparative study. The results of the wave forces on the two types of bottom topography showed that there were no significant shifts of the wave forces over a simple slope. The wave forces over a slope were slightly affected by the submergence depth, similar to the results over a flat bottom with a relatively weak nonlinearity, i.e.,  $H/h = 0.10$ . However, the nonlinear wave evolutions above the plate, such as wave deformation, breaking and vortex generation at the leading or trailing edge of the plate, became dominant. As a result, the submergence depth and the bottom topography had no important influence on the nonlinear wave forces exerted on the plate.

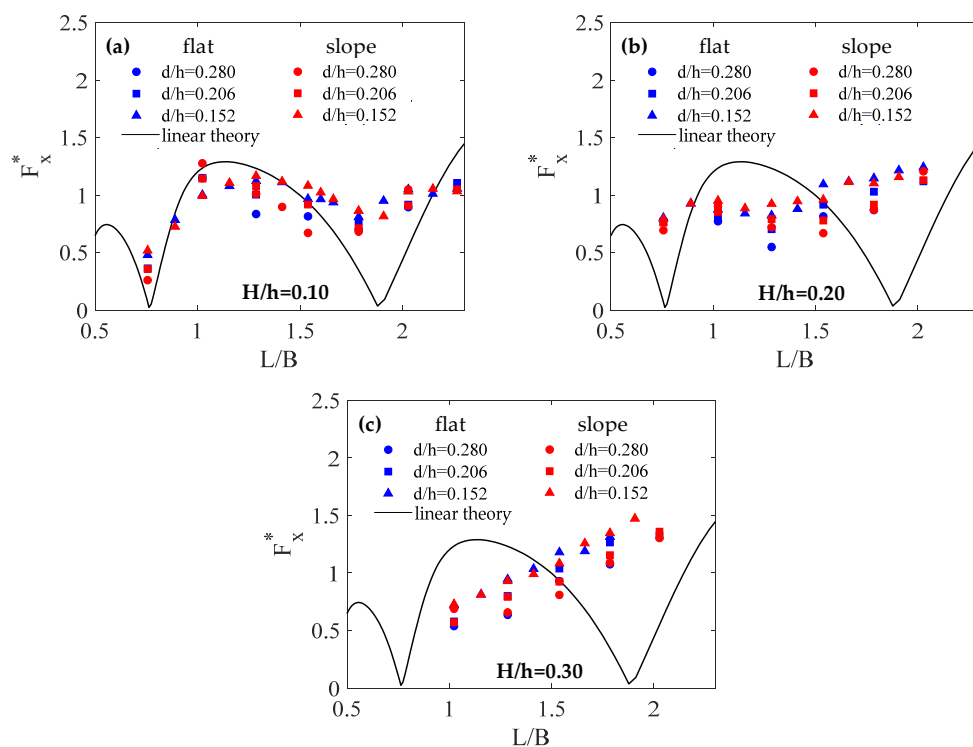


**Figure 7.** The horizontal wave forces due to regular waves in terms of the different relative wave heights (a)  $H/h = 0.10$ , (b)  $H/h = 0.20$  and (c)  $H/h = 0.30$ . The theoretical results from linear theory for flat bottoms are compared with the experimental data for both flat bottoms and slopes in the figure, as well as in Figures 8 and 9.

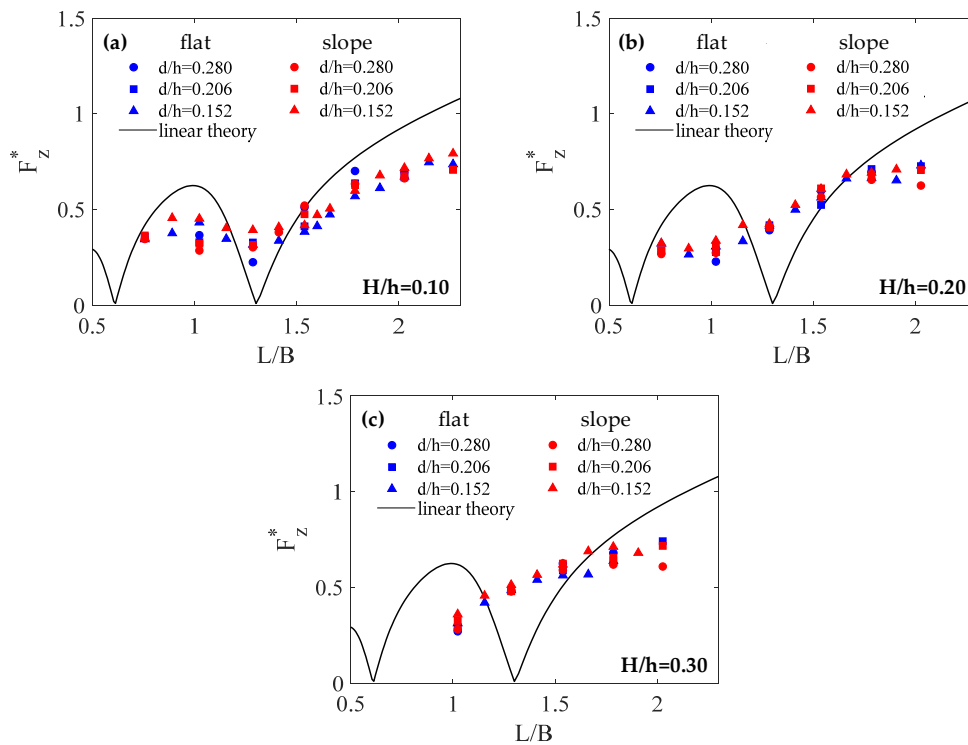


**Figure 8.** The vertical wave forces due to regular waves in terms of the different relative wave heights (a)  $H/h = 0.10$ , (b)  $H/h = 0.20$  and (c)  $H/h = 0.30$ .

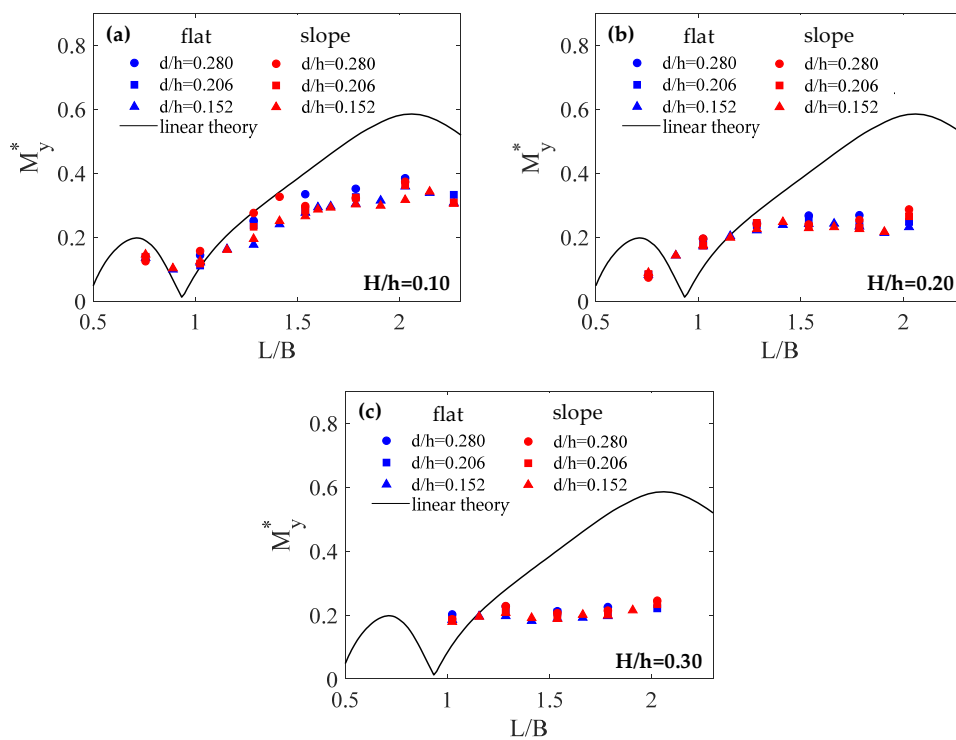


**Figure 9.** The overturning moments due to regular waves in terms of the different relative wave heights (a)  $H/h = 0.10$ , (b)  $H/h = 0.20$  and (c)  $H/h = 0.30$ .

#### 4.2. Solitary Waves

The wave scattering on a submerged horizontal plate due to a solitary wave had not been investigated by analytical methods until Lo and Liu [30] developed the solution for linear long waves. For solitary waves, the analytical solutions for a wave-scattering problem are formulated and obtained based on linear shallow-water wave theory as small-amplitude solitary waves can be theoretically generalized to long waves. Previous studies [10,30] showed that the theoretical solutions compared well with both the experimental and numerical data for small incident solitary waves in terms of the surface elevation, pressure along the plate and induced forces acting on the plate, and large discrepancies were observed for larger solitary wave heights, which is an expected limitation of the linear theory. In this paper, the analytical solutions were compared and examined against experimental data. In general, we found that the approximate solutions were essentially consistent in the leading edge, where the nonlinearity was not significant.

For the representative case, ( $H/h = 0.326$ ,  $d/h = 0.280$ ), the experimental and theoretical surface elevations are compared in Figure 10. In general, the measured surface elevations in the reflected region (WG1 and WG2) were basically consistent with the theoretical solutions, even though the incoming waves were of significant nonlinearity. Small oscillations in the tails of the waves were observed both in the experimental data and the linear theory. The oscillations may result from evanescent modes and nonlinearity, which are not accounted for in the linear theory. Significant discrepancies exist between the experimental data and linear solutions in the transmitted region (WG3 and WG4). We observed that wave breaking occurred in the transmitted region, which indicated higher nonlinearity caused by the submerged plate. The linear theory tended to underestimate the wave heights in the transmitted region.

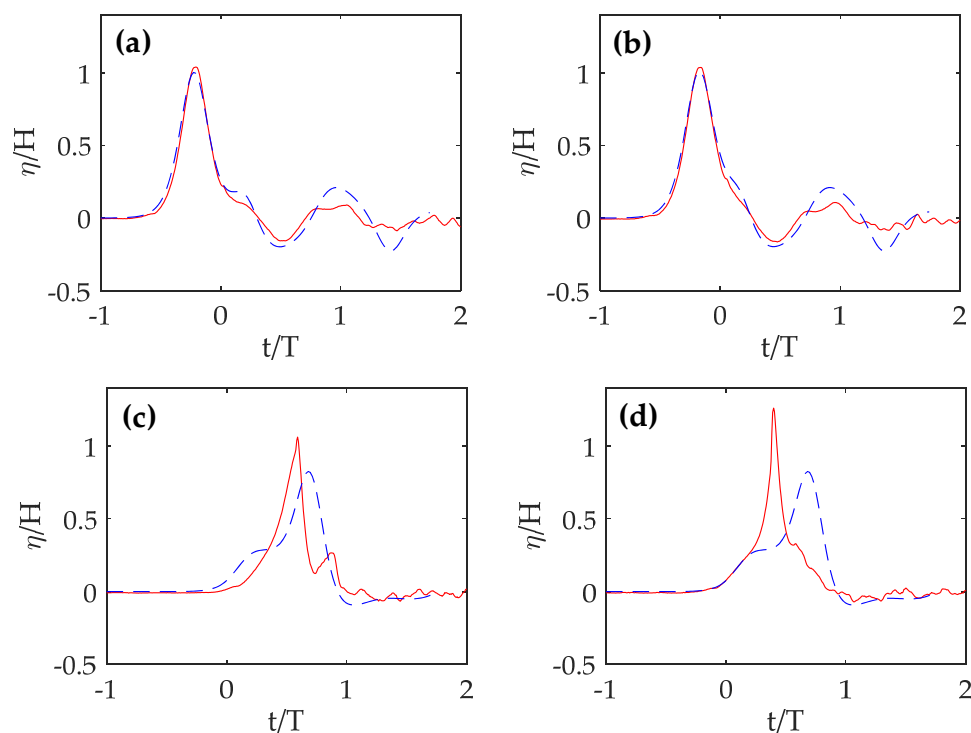


**Figure 10.** The time series of surface elevations in the front (a) WG1 and (b) WG2 and in the rear (c) WG3 and (d) WG4 of the plate over a flat bottom due to a solitary wave. ( $H/h = 0.326$ ,  $d/h = 0.280$ ).

Figure 11 illustrates the time series of exciting wave forces and overturning moments with the analytical results of the linear theory. This shows that the first peak of the vertical force and overturning moment were well predicted by the linear theory because the free surface had not yet

violently deformed before the wave front arrived at the leading edge of the plate. However, the linear theory overestimated the vertical forces and overturning moment after the first peak as a result of the nonlinearity and dissipation not accounted for in the linear theory. We found that the positive horizontal force was well predicted by the linear theory, while the negative horizontal forces showed a significant discrepancy between the experimental data and the theoretical results, as shown in Figure 11a.

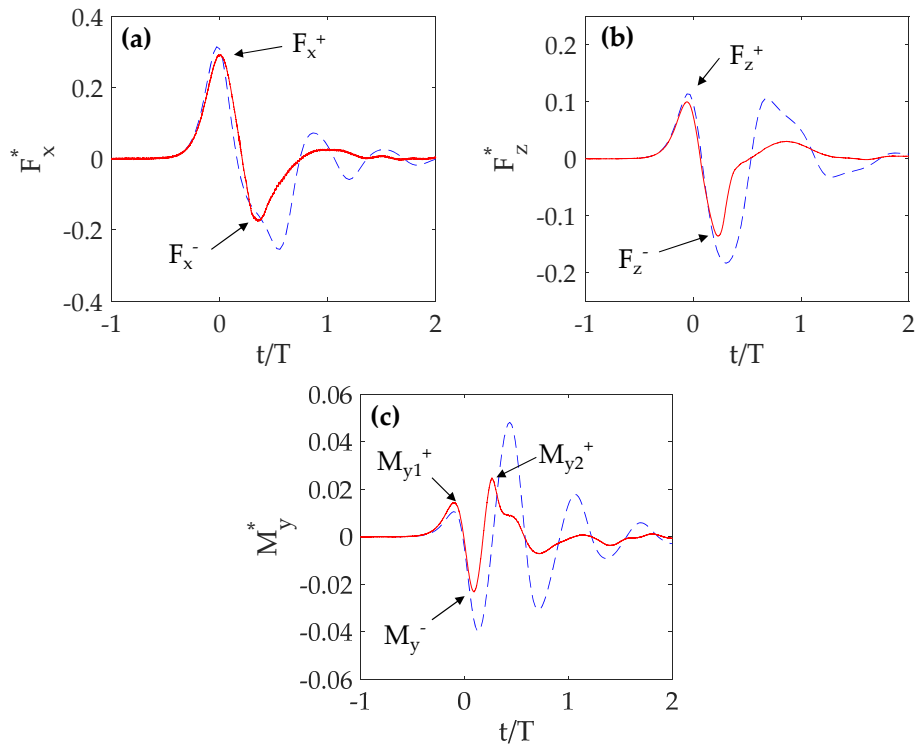


**Figure 11.** The time series of wave forces due to a solitary wave. ( $H/h = 0.326$ ,  $d/h = 0.28$ ). (a)  $F_x^*$ ; (b)  $F_z^*$ ; (c)  $M_y^*$ .

Under the linear long wave assumption, the pressure on the leading and trailing edges of the submerged plate were both uniform along the spanwise direction. However, in reality, the leading wave was significantly deformed at the trailing edge and a vortex with strong intensity was observed in the experiments, which indicates that the pressure at the trailing edge may be not described exactly by the linear theory. There were two crests and one trough in the curve of the overturning moment in the present experimental setup, and the second positive overturning moments were larger than the first ones. Dimensionless wave forces for solitary waves were deduced, which involved the water depth  $h$ , instead of the wave heights  $H$ , in Equation (6), as the solitary wave heights were considered as independent variables. For the dimensionless wave forces due to solitary waves, the positive overturning moments were distinguished as the first  $M_{y1}^+$  and the second  $M_{y2}^+$ , as shown in Figure 11c.

The effects of the relative wave heights are shown in Figure 12, in which solitary wave forces with different wave heights are plotted together. The wave forces clearly increased with larger incident wave heights. The wave forces were larger than the negative forces, while the positive vertical forces were slightly smaller than the negative forces on a flat bottom. The absolute values of the force maxima and minima are plotted in the figure with the relative solitary wave heights. In general, the wave forces of the three components increased with larger incident wave heights. The forward horizontal forces were larger than the backward forces, while the upward vertical forces were slightly smaller than the downward forces. We found that the horizontal forces increased linearly with the relative wave heights.

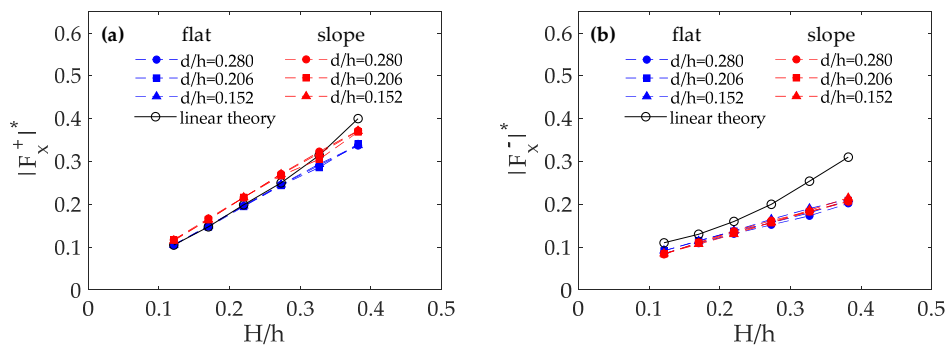


**Figure 12.** The horizontal wave forces due to solitary waves in terms of the different wave force components (a) positive horizontal wave force and (b) negative horizontal wave force. The theoretical results from linear theory for flat bottoms are compared with the experimental data for both flat bottoms and slope in the figure, as well as in Figures 13 and 14.

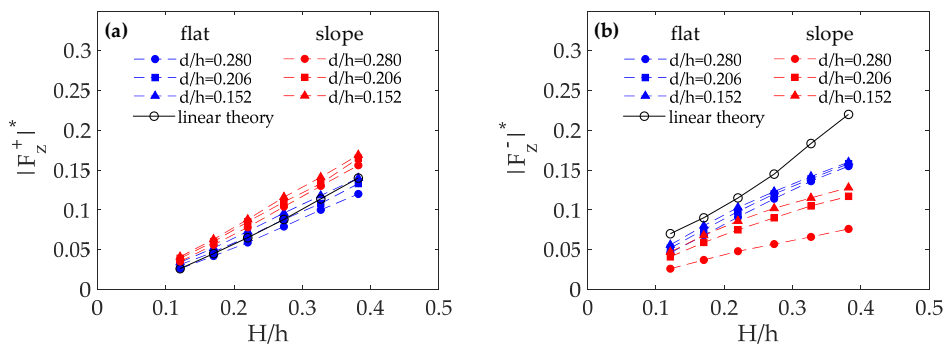


**Figure 13.** The vertical wave forces due to solitary waves in terms of the different wave force components (a) positive vertical wave force and (b) negative vertical wave force.

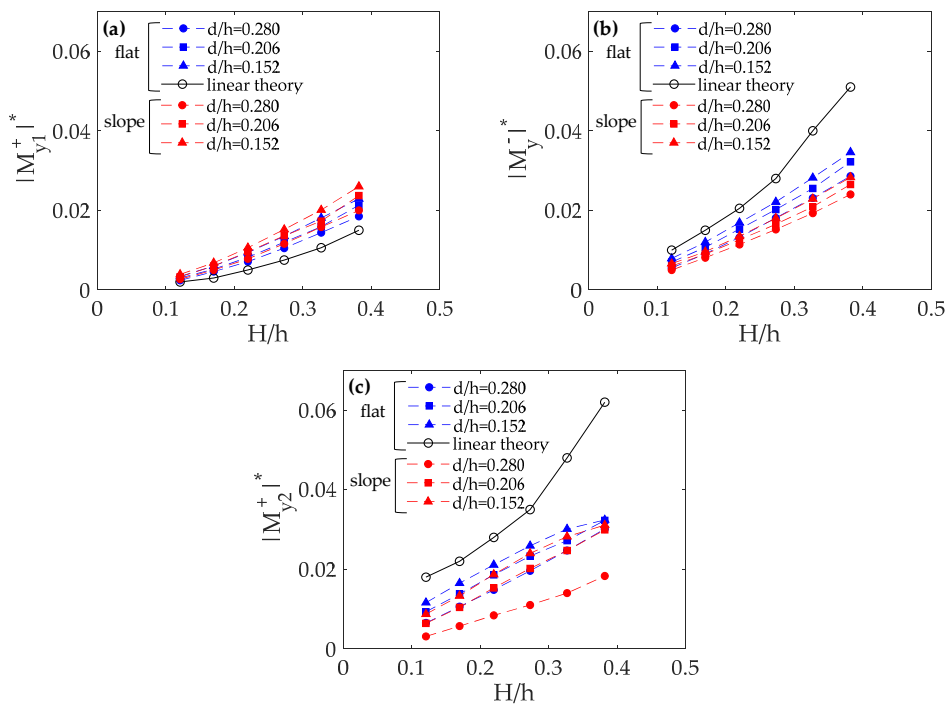


**Figure 14.** The overturning moments due to solitary waves in terms of the different wave force components (a) the first positive overturning moment, (b) the negative overturning moment and (c) the second overturning moment.

For the effect of submergence depth, we found that the horizontal forces were not influenced by the submergence depth, while the vertical forces and overturning moment were slightly affected by the submergence depth. Specifically, the vertical forces and overturning moments were larger when the submergence depth decreased. The peak values of the negative vertical force and the second positive overturning moment did not increase with the relative wave height because the wave height was so large (e.g.,  $H/h = 0.382$ ,  $d/h = 0.152$ ) that the wave had already broken after passing the plate.

Figures 13 and 14 shows comparisons of the solitary wave forces to the relative wave heights on a flat bottom and a 1:10 slope with different submergence depths. The wave forces that were affected by the sloped bottom were the negative vertical forces and the second positive overturning moment, which also depended on the submergence depth. The positive horizontal force slightly increased on a 1:10 slope, while no difference was observed for the negative horizontal force. The effects of the slope on the positive and negative vertical forces and overturning moment were inversed, namely,  $\{|F_z^+|^*$  and  $|M_{y1}^+|^*\}$  increased and  $\{|F_z^-|^*$ ,  $|M_y^-|^*$  and  $|M_{y2}^+|^*\}$  decreased. The wave forces on a 1:10 slope were closely related to the submergence depth, i.e., the wave forces decreased more with larger submergence depths. For example, the negative vertical forces and the second positive overturning moment decreased by 51% and 39% with  $H/h = 0.382$  and  $d/h = 0.280$ , respectively. This may be due to the different flow fields around the trailing edge on a simple slope. A higher velocity field and intense vortex were observed in the experiments, which may lead to the changes of wave forces, as discussed by others (e.g., Poupardin et al. [18]; Lo and Liu [30]).

## 5. Conclusions

A series of wave force experiments on a submerged horizontal plate with regular waves and solitary waves were performed on a flat bottom and a 1:10 simple slope. A dynamometric system in a wave flume was set up to measure the horizontal force, vertical force and overturning moment exerted on the structures. The experimental results on a flat bottom were presented and compared with the results based on the linear theory. The wave force dependences on the wave length, wave height, submergence depth and sloped topography were discussed.

For regular waves, the wave forces on a flat bottom essentially increased with the relative wave length until reaching a critical wave length where the wave forces no longer increased. The horizontal forces slightly decreased with the increasing submergence depth, while the vertical forces and the overturning moment were not changed with the submergence depth, especially with larger wave heights. The analytical results from the linear theory showed an agreement for small wave height ( $H/h = 0.10$ ) and relatively short wave length ( $L/B < 1.5$  in the present study). The wave forces differ significantly from the linear theory for larger waves over a flat bottom and a 1:10 simple slope. The influence of the bottom topography or the submergence depth was not important for the nonlinear wave forces exerted on the plate, compared with the nonlinear wave evolutions above the plate, such as the wave deformation, breaking and vortex generation at the leading and trailing edges of the plate.

For solitary waves, the linear long wave theory for a flat bottom provided reasonable predictions of the surface elevation in the reflected region, as well as the first peak of the vertical force and the overturning moment. The wave forces on a flat bottom increased distinctly with the relative wave height. The vertical force and the overturning moment became larger when the submergence depth decreased, while the horizontal force was not influenced by the submergence depth. The effects of a simple slope on the wave forces for solitary waves were related to the submergence depth. The main differences in the wave forces for the case of the 1:10 simple slope model were in terms of the negative vertical forces and the second positive overturning moment. The magnitude of these two terms decreased due to the existence of the slope.

**Author Contributions:** This paper was the result of collaborative teamwork. Experiment and data analysis, J.D.; Writing—original draft, J.D.; Writing—review and editing, J.S. and C.Z.; Supervision, L.X., K.C. and C.Z. All authors have read and agreed to the published version of the manuscript.

**Funding:** This research was funded by the Postdoctoral Foundation of Zhejiang Province of China.

**Acknowledgments:** This work was supported by the Key Laboratory of Hydrodynamics of the Ministry of Education of China. The authors also thank Tian Geng at University College Dublin for his technical support and helpful discussion.

**Conflicts of Interest:** The authors declare no conflict of interest.

## References

1. Heins, A.E. Water waves over a channel of finite depth with a submerged plane barrier. *Can. J. Math.* **1950**, *2*, 210–222. [[CrossRef](#)]
2. Ijima, T.; Ozaki, S.; Eguchi, Y.; Kobayashi, A. Breakwater and quay wall by horizontal plates. In Proceedings of the 12th Conference on Coastal Engineering, Washington, DC, USA, 13–18 September 1970; Volume 3, pp. 1537–1556.
3. Watanabe, E.; Utsunomiya, T.; Wang, C.M. Hydroelastic analysis of pontoon-type VLFS: A literature survey. *Eng. Struct.* **2004**, *26*, 245–256. [[CrossRef](#)]
4. Orer, G.; Ozdamar, A. An experimental study on the efficiency of the submerged plate wave energy converter. *Renew. Energy* **2007**, *32*, 1317–1327. [[CrossRef](#)]
5. Ning, D.; Zhao, X.; Goteman, M.; Kang, H. Hydrodynamic performance of a pile-restrained WEC-type floating breakwater: An experimental study. *Renew. Energy* **2016**, *95*, 531–541. [[CrossRef](#)]
6. Zhao, X.L.; Ning, D.Z.; Liang, D.F. Experimental investigation on hydrodynamic performance of a breakwater-integrated WEC system. *Ocean Eng.* **2019**, *171*, 25–32. [[CrossRef](#)]
7. Siew, P.; Hurley, D. Long surface waves incident on a submerged horizontal plate. *J. Fluid Mech.* **1977**, *83*, 141–151. [[CrossRef](#)]
8. Patarapanich, M. Maximum and zero reflection from submerged plate. *J. Waterw. Port. Coast. Ocean Eng.* **1984**, *110*, 171–181. [[CrossRef](#)]
9. Patarapanich, M.; Cheong, H.-F. Reflection and transmission characteristics of regular and random waves from a submerged horizontal plate. *Coast. Eng.* **1989**, *13*, 161–182. [[CrossRef](#)]
10. Cheong, H.-F.; Shankar, N.J.; Nallayarasu, S. Analysis of submerged platform breakwater by eigenfunction expansion method. *Ocean Eng.* **1996**, *23*, 649–666. [[CrossRef](#)]
11. Cheng, Y.; Ji, C.; Ma, Z.; Zhai, G.; Oleg, G. Numerical and experimental investigation of nonlinear focused waves-current interaction with a submerged plate. *Ocean Eng.* **2017**, *135*, 11–27. [[CrossRef](#)]
12. Patarapanich, M. Forces and moment on a horizontal plate due to wave scattering. *Coast. Eng.* **1984**, *8*, 279–301. [[CrossRef](#)]
13. Liu, P.L.-F.; Iskandarani, M. *Hydrodynamic Wave Forces on Submerged Horizontal Plate*; National Research Council Canada: Ottawa, ON, Canada, 1989; pp. C51–C64.
14. Rey, V.; Touboul, J. Forces and moment on a horizontal plate due to regular and irregular waves in the presence of current. *Appl. Ocean Res.* **2011**, *33*, 88–99. [[CrossRef](#)]
15. Yu, X.; Isobe, M.; Watanabe, A. Wave breaking over submerged horizontal plate. *J. Waterw. Port. Coast. Ocean Eng.* **1995**, *121*, 105–113. [[CrossRef](#)]
16. Kojima, H.; Yoshida, A.; Nakamura, T. Linear and nonlinear wave forces exerted on a submerged horizontal plate. *Coast. Eng. Proc.* **1994**, *1*, 1312–1326.
17. Liu, C.; Huang, Z.; Tan, S.K. Nonlinear scattering of non-breaking waves by a submerged horizontal plate: Experiments and simulations. *Ocean Eng.* **2009**, *36*, 1332–1345. [[CrossRef](#)]
18. Poupardin, A.; Perret, G.; Pinon, G.; Bourneton, N.; Rivoalen, E.; Brossard, J. Vortex kinematic around a submerged plate under water waves. Part I: Experimental analysis. *Eur. J. Mech. B/Fluids* **2012**, *34*, 47–55. [[CrossRef](#)]
19. Yu, X. Functional performance of a submerged and essentially horizontal plate for offshore wave control: A review. *Coast. Eng. J.* **2002**, *44*, 127–147. [[CrossRef](#)]
20. Brossard, J.; Perret, G.; Blonce, L.; Diedhiou, A. Higher harmonics induced by a submerged horizontal plate and a submerged rectangular step in a wave flume. *Coast. Eng.* **2009**, *56*, 11–22. [[CrossRef](#)]
21. Zhang, C.; Zhang, Q.; Zheng, J.; Demirbilek, Z. Parameterization of nearshore wave front slope. *Coast. Eng.* **2017**, *127*, 80–87. [[CrossRef](#)]
22. Li, X.; Ning, D.; Xiao, Q.; Mayon, R. Disintegration of nonlinear long waves over even and uneven bathymetry. *J. Coast. Res.* **2019**, *35*, 1285–1293. [[CrossRef](#)]

23. Hayatdavoodi, M.; Ertekin, R.C. Wave forces on a submerged horizontal plate–Part II: Solitary and cnoidal waves. *J. Fluids Struct.* **2015**, *54*, 580–596. [[CrossRef](#)]
24. Hayatdavoodi, M.; Treichel, K.; Ertekin, R.C. Parametric study of nonlinear wave loads on submerged decks in shallow water. *J. Fluids Struct.* **2019**, *86*, 266–289. [[CrossRef](#)]
25. Dong, J.; Wang, B.; Zhao, X.; Liu, H. Wave forces exerted on a submerged horizontal plate over an uneven bottom. *J. Eng. Mech.* **2018**, *144*, 04018030. [[CrossRef](#)]
26. Xu, Y.; Zhang, G.; Wan, D.; Chen, G. MPS method for study of interactions between solitary wave and submerged horizontal plate. In Proceedings of the 29th International Society of Offshore and Polar Engineers, Honolulu, HI, USA, 16–21 June 2019.
27. Chu, C.R.; Chung, C.H.; Wu, T.R.; Wang, C.Y. Numerical analysis of free surface flow over a submerged rectangular bridge deck. *J. Hydraul. Eng.* **2016**, *142*, 04016060. [[CrossRef](#)]
28. Wang, Q.; Fang, Y.; Liu, H. An experimental study on wave loads on a submerged horizontal plate in solitary wave. In Proceedings of the 29th International Society of Offshore and Polar Engineers, Honolulu, HI, USA, 16–21 June 2019.
29. Jones, L.M.; Klamo, J.T.; Kwon, Y.W.; Didoszak, J.M. Numerical and experimental study of wave-induced load effects on a submerged body near the surface. In Proceedings of the 37th ASME International Conference on Ocean, Offshore and Arctic Engineering, Madrid, Spain, 25 September 2018.
30. Lo, H.Y.; Liu, P.L.-F. Solitary Waves Incident on a Submerged Horizontal Plate. *J. Waterw. Port Coast. Ocean Eng.* **2014**, *140*, 04014009.
31. Seiffert, B.; Hayatdavoodi, M.; Ertekin, R.C. Experiments and computations of solitary-wave forces on a coastal-bridge deck. Part, I: Flat plate. *Coast. Eng. J.* **2014**, *88*, 194–209. [[CrossRef](#)]
32. Hayatdavoodi, M.; Ertekin, R.C.; Valentine, B.D. Solitary and cnoidal wave scattering by a submerged horizontal plate in shallow water. *AIP Adv.* **2017**, *7*, 065212. [[CrossRef](#)]
33. Dong, J.; Wang, B.; Liu, H. Wave forces on a submerged horizontal plate over a sloping beach due to a solitary wave. In Proceedings of the 12th ISOPE Pacific/Asia Offshore Mechanics Symposium, Gold Coast, Australia, 4–7 October 2016.
34. Carmigniani, R.; Leroy, A.; Violeau, D. A simple SPH model of a free surface water wave pump: Waves above a submerged plate. *Coast. Eng. J.* **2019**, *61*, 96–108. [[CrossRef](#)]
35. He, M.; Gao, X.; Xu, W.; Ren, B.; Wang, H. Potential application of submerged horizontal plate as a wave energy breakwater: A 2D study using the WCSPH method. *Ocean Eng.* **2019**, 27–46. [[CrossRef](#)]
36. Ning, D.; Chen, L.; Lin, H.; Zou, Q.; Teng, B. Interaction mechanisms among waves, currents and a submerged plate. *Appl. Ocean. Res.* **2019**, *91*, 101911. [[CrossRef](#)]
37. Madsen, O.S.; Mei, C.C. The Transformation of a Solitary Wave over an Uneven Bottom. *J. Fluid Mech.* **1969**, *39*, 781–791. [[CrossRef](#)]
38. Dingemans, M.W. *Water Wave Propagation over Uneven Bottoms*; World Scientific Publishing: Singapore, 1997.
39. Mondal, R.; Takagi, K. Wave scattering by a fixed submerged platform over a step bottom. *Proc. Inst. Mech. Eng. Part M J. Eng. Marit. Environ.* **2019**, *233*, 93–107. [[CrossRef](#)]
40. Dhillon, H.; Banerjea, S.; Mandal, B.N. Water wave scattering by a finite dock over a step-type bottom topography. *Ocean Eng.* **2016**, 1–10. [[CrossRef](#)]
41. Dhillon, H.; Banerjea, S. Effect of Variable Bottom Topography on Water Wave Incident on a Finite Dock. In *Mathematics and Computing*; Springer Proceedings in Mathematics & Statistics; Mohapatra, R., Chowdhury, D., Giri, D., Eds.; Springer: New Delhi, India, 2015.
42. Malek-Mohammadi, S.; Testik, F.Y. New methodology for laboratory generation of solitary waves. *J. Waterw. Port. Coast. Ocean Eng.* **2010**, *36*, 286–294. [[CrossRef](#)]
43. Grimshaw, R.H.J. The solitary wave in water of variable depth. *J. Fluid Mech.* **1971**, *46*, 611–622. [[CrossRef](#)]

